HHS Public Access

Author manuscript

Cell Rep. Author manuscript; available in PMC 2019 January 29.

Published in final edited form as:

Cell Rep. 2019 January 15; 26(3): 564–572.e5. doi:10.1016/j.celrep.2018.12.084.

Binding of FANCI-FANCD2 Complex to RNA and R-Loops Stimulates Robust FANCD2 Monoubiquitination

Zhuobin Liang[1,3], **Fengshan Liang**[1,3], **Yaqun Teng**[4,5], **Xiaoyong Chen**[1], **Jingchun Liu**[1], **Simonne Longerich**[3], **Timsi Rao**[3], **Allison M. Green**[1,2], **Natalie B. Collins**[6], **Yong Xiong**[3], **Li Lan**[5,7,8], **Patrick Sung**[3,9,*], and **Gary M. Kupfer**[1,2,10,*]

[1]Department of Pediatrics, Yale Medical School, New Haven, CT 06520, USA

[2]Department of Pathology, Yale Medical School, New Haven, CT 06520, USA

[3]Department of Molecular Biology and Biophysics, Yale Medical School, New Haven, CT 06520, USA

[4]School of Medicine, Tsinghua University, No.1 Tsinghua Yuan, Haidian District, Beijing 100084, China

[5]Department of Microbiology and Molecular Genetics, University of Pittsburgh School of Medicine, Pittsburgh, PA 15219, USA

[6]Department of Pediatric Oncology, Dana-Farber Cancer Institute, Harvard Medical School, Boston, MA 02115, USA

[7]Massachusetts General Hospital Cancer Center, Harvard Medical School, Boston, MA 02129, USA

[8]Department of Radiation Oncology, Massachusetts General Hospital, Harvard Medical School, Boston, MA 02129, USA

[9]Department of Biochemistry and Structural Biology, University of Texas Health Science Center at San Antonio, San Antonio, TX 78229, USA

[10]Lead Contact

SUMMARY

Fanconi anemia (FA) is characterized by developmental abnormalities, bone marrow failure, and cancer predisposition. FA cells are hypersensitive to DNA replicative stress and accumulate co-transcriptional R-loops. Here, we use the Damage At RNA Transcription assay to reveal

*Correspondence: sungp@uthscsa.edu(P.S.), gary.kupfer@yale.edu(G.M.K.).

AUTHOR CONTRIBUTIONS

G.M.K., P.S., Z.L., F.L., Y.T., J.L., and L.L. conceived the experiments and analyzed the data. Z.L., F.L., Y.T., X.C., J.L., S.L., T.R., A.G., and N.B.C. performed the experiments. Z.L., G.M.K., and P.S. wrote the manuscript.

SUPPLEMENTAL INFORMATION

Supplemental Information includes four figures and one table and can be found with this article online athttps://doi.org/10.1016/j.celrep.2018.12.084.

DECLARATION OF INTERESTS

The authors declare no competing interests.

colocalization of FANCD2 with R-loops in a highly transcribed genomic locus upon DNA damage. We further demonstrate that highly purified human FANCI-FANCD2 (ID2) complex binds synthetic single-stranded RNA (ssRNA) and R-loop substrates with high affinity, preferring guanine-rich sequences. Importantly, we elucidate that human ID2 binds an R-loop structure via recognition of the displaced ssDNA and ssRNA but not the RNA:DNA hybrids. Finally, a series of RNA and R-loop substrates are found to strongly stimulate ID2 monoubiquitination, with activity corresponding to their binding affinity. In summary, our results support a mechanism whereby the ID2 complex suppresses the formation of pathogenic R-loops by binding ssRNA and ssDNA species, thereby activating the FA pathway.

Graphical Abstract

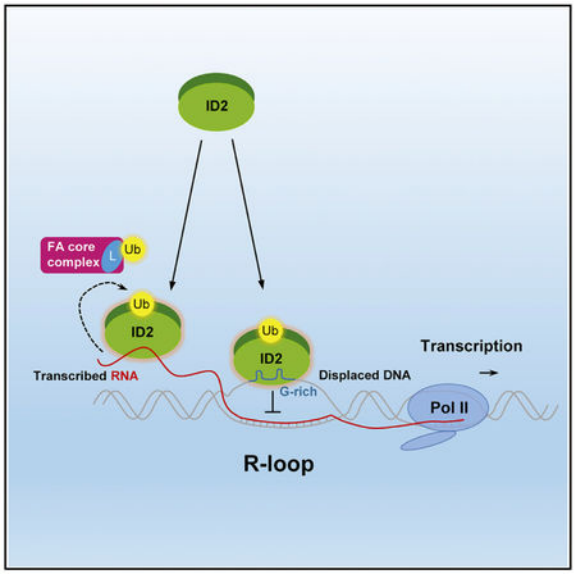

In Brief

Fanconi anemia pathway has a well-known role in the repair of DNA crosslinks, but its recently identified role in suppression of co-transcriptional R-loops remains elusive. Here, Liang et al. show that FANCI-FANCD2 has intrinsic RNA and R-loop binding activity and provide mechanistic insights into FA pathway activation upon transcription stress.

INTRODUCTION

Fanconi anemia (FA) is a recessive genetic disorder characterized by congenital abnormalities, bone marrow failure, and a strong predisposition to cancer. FA is a multigenic disease, with at least 22 complementation genes (*FANCA-FANCV*) having been identified thus far, which, together with other partner proteins, constitute the FA pathway of DNA damage sensing and repair (Nalepa and Clapp, 2018). The FA core complex harbors the ubiquitin E3 ligase FANCL and catalyzes the monoubiquitination of the FANCI-FANCD2 (ID2) heterodimer complex during S phase and upon occurrence of interstrand DNA crosslinkings (ICLs) and replicative stress (Huang et al., 2014; Rajendra et al., 2014; van Twest et al., 2017). The monoubiquitinated ID2 complex stably associates with damaged

DNA, where it is thought to nucleate the formation of repair centers that harbor a number of other FA proteins involved in ICL removal and subsequent DNA repair including SLX4/FANCP, BRCA1/FANCS, BRCA2/FANCD1, BACH1/FANCJ, and PALB2/FANCN (Cantor et al., 2001; Godthelp et al., 2006; Kim et al., 2011; Xia et al., 2007). Importantly, mutation of the ubiquitin acceptor site in FANCD2 impairs the assembly of DNA repair foci comprising the aforementioned FA proteins (Chen et al., 2014; Wang et al., 2004; Yamamoto et al., 2011). Thus, ID2 monoubiquitination represents a pivotal event in the activation of the FA pathway.

Previous studies demonstrated that *in vitro* monoubiquitination of purified FANCI and ID2 by FANCL-UBE2T is greatly stimulated upon DNA binding (Longerich et al., 2009, 2014; Sato et al., 2012), which can cause a conformational change of ID2 revealing the concealed monouniquition sites (Joo et al., 2011; Liang et al., 2016). In addition, ID2 exhibits binding preference for DNA substrates that mimic intermediates of a stalled replication fork underlying the physiological relevance of ID2 DNA binding in ICL repair.

To further characterize the FA pathway in mitigating conflict of DNA replication and RNA transcription upon DNA damage, recent studies have revealed roles of several FA factors including FANCD2, FANCA, BRCA1/FANCS, and BRCA2/FANCD1 in the metabolism of R-loops, which contain RNA:DNA hybrids that can interfere with DNA replication and can result in DNA double-strand breaks and genome instability (Bhatia et al., 2014; García-Rubio et al., 2015; Hatchi et al., 2015; Schwab et al., 2015).

In this study, we confirm the presence of increased R-loops in FA mutant cells, as previously reported (García-Rubio et al., 2015; Schwab et al., 2015), show that FANCD2 monoubiquitination is required to prevent their accumulation and demonstrate that FANCD2 colocalizes with R-loops in an actively transcribed genomic region. We also demonstrate that purified recombinant human ID2 can directly bind RNA with a predilection for single-stranded and high-guanine-content RNA, as well as R-loop structures. Importantly, these same RNA and R-loop species are able to stimulate robust monoubiquitination of ID2 complex in a reconstituted system. Taken together, our results provide direct evidence for RNA-mediated ID2 monoubiquitination in the avoidance of genome instability that is induced by the accumulation of pathogenic R-loops.

RESULTS

FANCD2 Colocalizes with R-Loops at a DNA Damaged, Actively Transcribed Genomic Site

Recent work has demonstrated that the FA pathway has a role in preventing R-loop accumulation upon replication and transcription stress (García-Rubio et al., 2015; Schwab et al., 2015). In order to confirm these data, we compared FA-D2 mutant cells with absent FANCD2 expression transduced with different FANCD2 expression constructs and found that cells expressing FANCD2 monoubiquitination-dead FANCD2-K561R mutant (FA-D2+K561R) or vector alone had elevated background level of R-loops as visualized by S9.6 immunofluorescence microscopy, which further accumulated over the time-course of DNA cross-linking agent mitomycin C (MMC) treatment (Figures S1A and S1B). Conversely, expression of RNA:DNA endonuclease RNase H1 markedly reduced S9.6 signal and

partially rescued the survival of FA-D2 mutant cells in MMC (Figures S1C–S1E). Nondenaturating bisulfite sequencing also demonstrated increased R-loops at the highly transcribed GAPDH gene in cells defective in FANCD2 monoubiquitination (Figure S1F). Collectively, our results demonstrate that ID2 and its monoubiquitination facilitate R-loop avoidance upon replication stress, confirming previously published results (García-Rubio et al., 2015; Schwab et al., 2015).

To understand how transcription influences recruitment and activation of ID2 to prevent co-transcriptional R-loops, we deployed the DNA Damage At RNA Transcription (DART) system to examine the association of FANCD2 (and by implication, ID2) with transcription upon DNA damage. DART utilizes the light-inducible chromophore-modified KillerRed (KR) to generate reactive oxygen species (ROS) at a genome-integrated tet response element (TRE) locus to induce focal DNA damage (Lan et al., 2014; Wei et al., 2015). The transcriptional status of the TRE locus can be modulated by fusion of KR with either transcription activator (TA) or repressor (tetR) (Figure 1A).

We first tested FANCD2 recruitment to the TRE locus in four combinations of transcription status and DNA damage by expressing different effector proteins. FANCD2 became highly enriched at the TRE locus when constitutively active transcription was stalled by ROS-induced DNA damage (TA-KR) but not in cells with only active transcription (TA-Cherry), only DNA damage (tetR-KR), or no transcription and DNA damage (tetR-Cherry) (Figures 1B and 1C). This result clearly supports the idea that both transcription and DNA damage are required to recruit FANCD2 (ID2) to chromatin for its subsequent monoubiquitination to form foci, consistent with a similar observation reported recently that endogenous FANCD2 colocalizes with large transcription units in response to aphidicolin-induced replication stress (Okamoto et al., 2018).

We hypothesized that perturbation of active transcription by ROS damage in TA-KR cells would lead to R-loop accumulation. Indeed, we observed that the TA-KR site was an R-loop hotspot as indicated by the formation of S9.6 foci in a transcription and DNA damage dependent fashion (Teng et al., 2018). Importantly, enriched foci of FANCD2 and S9.6 colocalized in ~75% of the TA-KR positive cells tested, and ~96% of the cells with distinct S9.6 foci at the TRE locus were positive for colocalized FANCD2 foci (Figures 1D and 1E). Furthermore, overexpression of wild-type RNase H1, but not the nuclease-dead RNase H1-D210N mutant, in TA-KR positive cells drastically diminished FANCD2 foci intensity at the TRE locus (Figures 1F and 1G), indicating that FANCD2 enriches at DNA-damaged, transcriptionally active genomic sites in a manner that depends on R-loops. In addition, small interfering RNA (siRNA) depletion of endogenous FANCD2 significantly increased S9.6 foci intensity at the TRE locus in TA-KR positive cells to a similar extent as the depletion of RNA helicase Aquarius (AQR) (Figures 1H and 1I), which is known to resolve R-loops (Sollier et al., 2014), demonstrating the utility of the DART system to study R-loop metabolism.

Human FANCI-FANCD2 Complex Binds Single-Stranded RNA but Not RNA:DNA Hybrids

Given that FANCD2 colocalizes with R-loops in cells, we asked whether ID2 complex possesses RNA binding activity. We first tested several biotinylated oligomers for their

ability to pull down FANCD2 from FA-D2 mutant cells transduced with either wild-type FANCD2 or FANCD2-K561R. Both FANCD2 and FANCI from cell extracts associated with RNA similarly as with DNA, and FANCD2 monoubiquitination is dispensable for RNA interaction as the K561R mutant can be pulled down also (Figures S2A and S2B). The majority of FANCD2 that was pulled down is not ubiquitinated even after MMC treatment, confirming that ubiquitination is indeed not required for RNA interaction. To investigate whether FANCD2 association with RNA could have nucleotide sequence preference, we tested RNA homopolymers for pull-down of FANCD2 and found that poly-rG has the highest pull-down efficiency (Figure S2C), suggesting RNA binding of FANCD2 may have a preference for guanine-rich sequences, which are often present in co-transcriptional R-loops.

In order to directly test RNA interaction of ID2 with RNA, we purified the human ID2 complex from insect cells (Figure 2A) and tested for RNA binding activity using the electrophoretic mobility shift assay (EMSA). We first examined a set of DNA and RNA substrates with the same nucleotide sequence in both single-stranded (ss) and double-stranded (ds) forms (Table S1). We observed that ID2 had significantly higher affinity for the tested ssRNA over ssDNA (Figure 2B). Unexpectedly, despite the fact that human ID2 bound ssRNA avidly, it had the lowest binding affinity for duplex substrates containing at least one RNA strand, such as dsRNA and RNA:DNA hybrids, while it bound dsDNA with a similar affinity as ssDNA (Figure 2C). Taken together, the order of human ID2 binding affinity from high to low in our experiments was ssRNA > ssDNAz≈dsDNA > dsRNAz≈RNA:DNA hybrids (Figure 2D).

We previously reported that FANCI DNA binding mutants in complex with wild-type FANCD2 can impede the DNA binding activity of ID2 (Longerich et al., 2009). To test whether ID2 shares the same dependence on FANCI in binding RNA, we tested the FANCI (KKEE)/D2 and FANCI (R1285X)/D2 mutants (Figure S2D), which are both impaired for DNA binding, for the ability to bind RNA. Our results showed that both ID2 mutant complexes were also defective in binding RNA (Figures S2E and S2F). To investigate the contribution of each subunit of the ID2 complex toward RNA binding activity, we first tested purified human FANCI and found it binds ssRNA, dsRNA, and RNA:DNA hybrids (Figures S3A and S3B). We were not able to test human FANCD2 protein alone, because, in the absence of FANCI, FANCD2 forms high-molecular-weight aggregates during purification. Instead, we took advantage of chicken FANCI and FANCD2 proteins, which can be purified in a non-aggregated form either alone or as a heterodimer, and found that ID2, FANCI, and FANCD2 all have strong binding activity toward ssRNA, dsRNA, and RNA:DNA hybrids (Figures S3C–S3H). These results confirm the findings of a recent study showing that purified chicken FANCI, FANCD2, and ID2 complex can bind RNA:DNA hybrids with high affinity (Okamoto et al., 2018). Taken together, our results suggest that while FANCI and FANCD2 both have strong affinity for RNA, the RNA binding activity of ID2 depends on the FANCI nucleic acid binding motif.

Guanine Content of RNA Positively Regulates Binding by ID2

We noted that FANCD2 preferentially interacted with RNA poly-rG in the pull-down assay (Figure S2C). To quantify the effect of the guanine content of nucleic acids on their binding by ID2, we compared three 60-mer ssDNA and ssRNA substrates with varying percentages of guanine content (see Table S1 for sequence information). These substrates are termed here as G8, G28, and G48 based on their guanine content. G28 is the same sequence used in Figure 2B, while G8 is derived from G28 by converting some G bases to A or T and G48 is derived from G28 by converting some A or T bases to G. As predicted, increasing the guanine content of both DNA and RNA enhanced their binding by ID2, and ID2 showed stronger affinity for ssRNA as compared to ssDNA of the same sequence among these tested substrates (Figures 2E–2H). In addition, we also observed similar effect of guanine content on human ID2 binding of dsDNA and dsRNA, despite dsRNA binding was weaker, as expected (Figures S3I–S3L).

FANCI-FANCD2 Complex Binds R-Loops via the Displaced ssDNA Strand and ssRNA Tail

To test ID2 for the ability to recognize R-loops, we first prepared a synthetic R-loop structure by hybridizing a guanine-rich RNA strand to a DNA bubble scaffold and compared ID2 binding to it versus a D-loop substrate of the same sequence. Our results showed that the R-loop substrate was bound by ID2 to the same extent as the D-loop (Figures S4A and S4B). Replacing the RNA:DNA hybrid portion of the R-loop to a A:T-rich sequence that has almost no binding affinity to ID2 based on our previous observations (Longerich et al., 2014) actually slightly increased the overall binding affinity (Figures S4C and S4D), suggesting that human ID2 R-loop binding occurs not via recognition of the RNA:DNA hybrids, consistent with our finding that human ID2 complex has poor binding affinity to RNA:DNA hybrids (Figure 2C).

R-loop binding of ID2 could be dependent on the displaced ssDNA strand and influenced by its guanine content and secondary structure. To address these questions, we constructed a series of R-loop substrates with different guanine contents in the displaced DNA strand and found that the R-loop binding affinity of ID2 positively correlates with the guanine content of the displaced ssDNA (Figures 3A and 3D). We also tested an R-loop substrate with the potential to form G-quadruplex, a frequent secondary structure found in the displaced ssDNA strand of R-loops and observed slight enhancement of binding affinity over the control R-loop with the same guanine content but without the G-quadruplex forming sequence (Figures 3B and 3D). Because ID2 robustly bound ssRNA, we hypothesized that another binding site of ID2 to an R-loop could be the ssRNA tail from a dysregulated mRNA transcript. To test this possibility, we synthesized additional R-loop substrates that harbor a 40-nt ssRNAtail at the 5′ end and observed that the additional ssRNA tail markedly increased R-loop ID2 binding affinity (Figures 3C and 3D). Furthermore, comparison of G-rich ssRNA and R-loop in a series of competition EMSA assays showed ID2 associating with both substrates robustly, with slightly higher affinity in ssRNA over R-loop for the substrates we tested (Figures S4E–S4H). Collectively, these results demonstrated that both the ssRNA and ssDNA moieties of a synthetic R-loop are critical components for recognition by ID2, thus implicating them in the recruitment and/or retention of ID2 at pathological R-loops in cells.

RNA and R-loop Support ID2 Monoubiquitination

Here, we asked whether RNA would similarly support FANCD2 monoubiquitination as DNA in a reconstituted *in vitro* ubiquitination system containing the E2-E3 enzymatic pair UBE2T and FANCL proteins. We found that ssRNA with a random sequence stimulated FANCD2 monoubiquitination to the same extent as the equivalent ssDNA counterpart, whereas poly-U (RNA) and poly-T (DNA) had little or no effect (Figure 4A), consistent with their weak binding affinity to ID2. As expected, ID2 complex containing FANCI DNA and RNA binding mutations failed to support ID2 monoubiquitination (Figure 4B). Indeed, the same set of DNA, RNA substrates used in EMSA all stimulated the monoubiquitination of FANCD2 in a manner consistent with their individual binding affinity (Figures 4C and 4D). As expected, R-loop substrates to which ID2 bound with high affinity stimulated FANCD2 monoubiquitination robustly (Figures 4E and 4F).

DISCUSSION

While the FA pathway has a well-known role in sensing and orchestrating the repair of DNA crosslinks, its recently described role in suppression or resolution of R-loops remains to be defined. In this study, we report findings of RNA and R-loop binding by ID2 and provide mechanistic insights of FA pathway activation in response to transcription stress. First, we show FANCD2 colocalizes with R-loops in cells and is able to bind ssRNA with G-rich sequence and R-loop structures with high affinity. Furthermore, our data provide experimental support that ID2 binds R-loops via recognition of the inherent single-stranded nucleic acid species, including the displaced DNA and unhybridized RNA. Importantly, we have shown that RNA and R-loop binding can stimulate robust ID2 monoubiquitination.

Based on these findings and current knowledge, we propose a model in which ID2 is recruited not only to sites of DNA damage such as the ICL, but also to transcription perturbed sites with accentuated R-loops (Figure 4G). We speculate that ID2 recruitment to R-loop, like to ICL, is dependent on the activity of the FA core complex proteins. This notion is supported by recent findings that showed assembly of the majority of FANCD2 foci requires R-loops (García-Rubio et al., 2015) and FANCD2 foci diminish upon depletion of FANCA (Okamoto et al., 2018). Furthermore, we suggest that ID2 monoubiquitination facilitates R-loop resolution via the recruitment of downstream factors. These factors could include nucleases, helicases, topoisomerases, RNA binding proteins, and DNA repair factors that have been implicated in either preventing the accumulation of pathological R-loops or in the resolution of these structures (Santos-Pereira and Aguilera, 2015). For example, the tumor suppressor BRCA1 has been shown to interact with the putative RNA helicase Senataxin (SETX), and the resulting complex localizes to R-loops (Hatchi et al., 2015). BRCA2 and its binding partner TREX also colocalize to R-loops (Bhatia et al., 2014). Finally, FANCM has been proposed to eliminate R-loops via its RNA:DNA helicase activity (Hodson et al., 2018; Schwab et al., 2015). We note that chromatin recruitment of BRCA1, BRCA2, and RAD51 upon replication stress depends monoubiquitination of ID2 (Garcia-Higuera et al., 2001; Taniguchi et al., 2002; Tripathi et al., 2016), which emphasizes a likely pivotal role of ID2 monoubiquitination in the recruitment and/or activation of factors that function in R-loop metabolism.

One unexpected finding of our study is that human ID2 has only weak affinity for RNA:DNA hybrids without any single-stranded characteristics. We speculate this may avoid inappropriate activation of the FA pathway in human cells where R-loops serve an important function in gene expression regulation (Skourti-Stathaki and Proudfoot, 2014). While the exact mechanism of such substrate recognition of human ID2 warrants further investigation, differences in primary protein sequences of FANCI and FANCD2 among vertebrates (Joo et al., 2011) support the notion that human ID2 might have evolved additional layers of nucleic acid recognition modules that are absent in ID2 homologs of lower vertebrates.

The preference of ID2 for guanine-rich DNA and RNA species likely reflects the higher propensity for such sequences to form secondary structures, which hints at the possibility that ID2 has specific affinity for these structures in its nucleic acid targets. Indeed, FANCD2 has been shown to associate with fragile genomic regions with strong and large transcriptional units (Madireddy et al., 2016; Okamoto et al., 2018), where genomic secondary structures stemming from aberrant DNA replication and transcription intermediates accentuate (Wilson et al., 2015). We also speculate that both FANCI and FANCD2 subunits contribute to the recognition of guanine-rich sequences based on the observation of similar binding activity using chicken proteins (Figure S3).

Our data add credence to the premise that any failure to prevent the formation of pathological R-loops or in the resolution of these structures contributes to the genomic instability seen in FA cells. Based on the phenotypic similarities shared by FA and other genetic diseases marked by aberrant RNA metabolism such as dyskeratosis congenita (DC), Diamond Blackfan anemia (DBA), and Shwachman-Diamond syndrome (SDS) (Dokal and Vulliamy, 2010), it is possible that R-loop formation leads to genomic instability seen in other cancer predisposition syndromes as well.

STAR★METHODS

CONTACT FOR REAGENT AND RESOURCE SHARING

Further information and requests for resources and reagents should be directed to and will be fulfilled by the Lead Contact, Gary M Kupfer (gary.kupfer@yale.edu).

EXPERIMENTAL MODEL AND SUBJECT DETAILS

Mammalian cell lines—FANCD2 deficient PD20 cells (GM16756, Coriell Institute, male) was used as the initial FA-D2 cell line to construct derivative PD20+pMMP-vector (FA-D2), PD20+pMMP-Flag-K561R (FA-D2+K561R) ubiquitination mutant, and PD20+pMMP-Flag-FANCD2 (FA-D2+FANCD2) wild-type cells. Cells were maintained at 37°C in a 5% CO_2 incubator and cultured in Dulbecco's modified Eagle medium (DMEM,Thermo Fisher) containing 10% fetal bovine serum (FBS, Biowest) and 1% Pen-Strep (Thermo Fisher). Cells stably transfected with pEGFP-N1-RNASEH1 (gift of James Manley, Columbia) and pEGFP-N1 empty vector were cultured in DMEM containing 10% FBS, 1% Pen-Strep, and 400 μg/ml G418 (Sigma). U2OS TRE cells (female) used in DART assay were cultured in dark at 37°C in a 5% CO_2 incubator using DMEM (Lonza) with 10%

FBS (GEMINI Bio-product). Mouse hybridoma cell line (HB-8730, ATCC, sex unknown) was used to purify S9.6 antibody.

Insect cell lines—Sf9 insect cells (Thermo Fisher) were used to produce initial baculoviruse and High Five insect cells (Thermo Fisher) were used as the host for protein expression.

BACTERIA STRAINS—Rosetta(DE3) pLysS was used as the strain for protein expression and DH5a (NEB) was used as the strain for plasmid cloninig.

METHOD DETAILS

Damage At RNA Transcription (DART) assay—The DART system has been described in previous publications (Lan et al., 2014; Wei et al., 2015). Briefly, the KillerRed (KR) or mCherry fusion protein expression vectors TA-KR, tetR-KR, TA-Cherry or tetR-Cherry in pBroad3 backbone were transfected into genetically engineered U2OS TRE cells in 35 mm glass-bottom dishes (MatTek). To introduce RNase H1 in the DART system, HA-RNase H1 (WT) or HA-RNase H1 (D210N) (Nguyen et al., 2017) was co-transfected with TA-KR. To induce DNA damage by KillerRed, cells that had been cultured in the dark for 36-48 hours were exposed to light (15 W Sylvania cool white fluorescent bulb) for 30 minutes and allowed to recover for 1 hour. For S9.6 foci staining, cells were then treated with 75 mM KCl (pre-warmed to 37°C) for 10 minutes and fixed by freshly made methanol-acetic acid (3:1) overnight, followed by 3 washes in PBS and steaming in TE buffer (10 mM Tris-HCl, 2 mM EDTA, pH 9.0) on a 95°C heating block for 20 minutes to expose the antigen. Next, cells were cooled, washed 3 times in PBS and blocked by 5% bovine serum albumin (BSA) (Sigma) in 0.1% PBS-Tween (PBST) for 1 hour at room temperature. S9.6 primary antibody (ENH001, Kerafast) and goat anti-mouse Alexa Fluor 488 or 405 secondary antibody (A-11001 or A-31553, Thermo Fisher) were used. For staining of endogenous FANCD2 foci in DART system, cells were rinsed in PBS and fixed in 4% paraformaldehyde (Affymetrix) for 15 minutes at room temperature. They were then washed 3 times by PBS, permeabilized by 0.2% Triton X-100 in PBS for 10 minutes, washed 3 times in PBS, and blocked by 5% BSA in 0.1% PBS-T for 30 minutes at room temperature. Primary FANCD2 antibody (sc-20022, Santa Cruz) was diluted in blocking buffer and incubated with cells overnight at 4°C. The cells were then washed 3 times in 0.05% PBS-T and incubated with goat anti-mouse Alexa Fluor 488 secondary antibody for 1 hour at room temperature. Finally, they were washed 3 times by 0.05% PBS-T and imaged in PBS. For co-staining with S9.6 and anti-FANCD2 in TA-KR cells, the method was the same as above for staining of S9.6 foci, and rabbit FANCD2 (A302-174A, Bethyl) antibody was added, followed by goat anti-rabbit Alexa Fluor 488 secondary antibody (A-11008, Thermo Fisher). For co-staining of FANCD2 and HA-RNase H1, the method was the same as staining of endogenous FANCD2 foci, and mouse HA antibody (11583816001, Roche) was added, followed by goat anti-mouse Alexa Fluor 405 secondary antibody. Images were acquired using the Olympus FV1000 confocal microscopy system. The foci intensity was directly measured by arbitrary unit from the ImageJ 1.50i software.

Immunofluorescence staining of RNA:DNA hybrids—For staining of RNA:DNA hybrids in FA-D2 cell lines, S9.6 antibody was purified from the mouse BALB/c hybridoma cells (gift of Tae Hoon Kim, Yale University) using NAb Protein A/G Spin Kit (Thermo Fisher) according to the manufacturer's instructions. Cells were plated in 8 chamber slides, grown to 50% confluence, and then treated with 500 nM MMC (Sigma) for the indicated time. Slides were then rinsed in PBS, fixed in 4% paraformaldehyde in PBS for 5 minutes, rinsed in PBS again, permeabilized in 0.5% Triton X-100 in PBS for 5 minutes, rinsed in PBS once more, and then blocked in PBS with 0.5% BSA, 0.1% NP-40 and 10% normal goat serum overnight at 4°C. Blocking agent was aspirated, and 1 μg/ml of S9.6 antibody in PBS with 0.1% NP-40 and 0.5% BSA was added to the slides, followed by an overnight incubation at 4°C. Slides were then washed three times in 0.1% PBS-T, and goat anti-mouse Alexa Fluor 555 secondary antibody (A-21422, Thermo Fisher) diluted 1:1000 was added to slides for 2 hours at room temperature. After washing 3 times in 0.1% PBS-T and 2 more times in PBS, slides were mounted using DAPI Vectashield Hard-Set (Vector Laboratories) and images were captured in a TE2000-E Eclipse inverted fluorescent microscope (Nikon). Volocity software (Perkin Elmer) was used to quantify immunofluorescence.

Cell survival assay—Cells were seeded into 6-well plates at 3,000 cells per well and incubated at 37°C for 24 hours. After the addition of MMC (Sigma), cell were incubated at 37°C for 5 days. Surviving cells were fixed in 10% methanol/10% acetic acid and stained with crystal violet solution (1% in methanol) for 5 minutes at room temperature on a rocker. Plates were then rinsed in water and allowed to dry, and crystal violet dye was extracted with 0.1% SDS in methanol for 1 hour at room temperature. Dye concentration was measured in a microplate reader (BioTek) by absorbance at 595 nm.

Nondenaturing bisulfite sequencing—R-loops were detected by using nondenaturing bisulfite treatment as previously reported (Yu et al., 2003). Briefly, genomic DNA was extracted by QIAGEN DNA Easy Kit and then treated with sodium bisulfite (Sigma) overnight at 37°C and purified. For the PCR reactions, the constitutively active glyceraldehyde 3-phosphate dehydrogenase (GAPDH) gene was amplified using the following primer pair, forward: 5′-GTCAAGGCTGAGAACGGGAA-3′; reverse: 5′-CTCCCCACATCACCCCTCTA-3′. The PCR products were then gel purified and Sanger-sequenced.

Biotinylated RNA pull-down—Cells were lysed in buffer containing 50mM Tris pH 7.5, 150mM NaCl, 1% Triton X-100, 1mM $MgCl_2$, and protease and phosphatase inhibitors (2 μg/ml aprotinin, 1 μg/ml pepstatin, 2 mg/ml leupeptin, 1 mM PMSF, 1 mM sodium pyrophosphate, and 1 mM Na_3VO_4). Cell suspensions were sonicated briefly and cleared by centrifugation, and protein concentration was determined by the Bradford assay (Pierce).Various amount of 60-mer biotinylated oligos (Keck Facility, Yale University) (5 ug in Figure S2A, 10 ug in Figure S2B and 2 ug in Figure S2C) were added to reaction buffer (10mM Tris pH 7.4, 1 mM DTT, 50 mM NaCl, 1 mM $MgCl_2$, 0.5 mM EDTA, 5% glycerol, and 1% DEPC) containing ~2 mg lysis proteins. After 2-hour incubation at 4°C, streptavidin resin (Pierce) was added, followed by another 2-hour incubation at 4°C. The resin was collected by centrifugation and washed 4 times in the reaction buffer. SDS loading buffer

was then added to resin and heated at 95°C for 5 minutes. Samples were subjected to standard immune blotting procedure described below.

Immunoblot analysis—Nitrocellulose membranes (Bio-Rad) were blocked in 5% milk in 0.1% PBS-T for 1 hour at room temperature, then incubated overnight at 4°C with diluted primary antibody. Membranes were washed three times in 0.1% PBS-T then incubated at room temperature for 1 hour with secondary antibody diluted 1:2000 in 0.5% milk in 0.1% PBS-T. Finally, membranes were washed five times in 0.1% PBS-T and developed by enzyme-linked chemiluminescence using Supersignal West Pico Kit (Pierce). GelQuant.NET (http://biochemlabsolutions.com/GelQuantNET.html) software was used to quantify intensity of bands in immunoblots. For immunoblotting, rabbit polyclonal FANCD2 antibody was obtained from Abcam (ab2187), rabbit polyclonal FANCI antibody was obtained from Bethyl (A301-254A), rabbit polyclonal RNase H1 antibody was obtained from Abcam (ab229078), and mouse monoclonal Ku86 antibody was obtained from Santa Cruz (sc-5280). ECL anti-rabbit (NA934) and anti-mouse (NA931) IgG HRP-linked secondary antibodies were obtained from Amersham Health.

Protein expression and purification—The human ID2 complex was expressed in insect cells and purified as previously described (Longerich et al., 2014; Longerich et al., 2009) with modifications. In brief, baculoviruses containing 6xHis-FANCI or 3xFlag-FANCD2 were generated by the Bac-to-Bac® Baculovirus Expression System (Thermo Fisher) following the manufacturer's manual. All the purification steps were carried out at 4°C. 800 mL High Five insect cells (1×10^6 cells/ml) were co-transfected with 1% (V/V) of fresh FANCI and FANCD2 recombinant baculoviruses for 40 hours, harvested and lysed in 20 mL Buffer A (25 mM Tris-Cl pH7.5, 10% Glycerol, 0.5 mM EDTA, 100 mM KCl, 0.01% IGEPAL, 1 mM DTT, 1 mM PMSF and protease inhibitors (5 μg/ml each of leupeptin, chymotrypsinogen, aprotinin, and pepstatin). The cell suspension was subjected to sonication with two 30 s pulses using a Branson 250 sonifier set to power 4.5, 50% output. The lysate was cleared by ultracentrifugation for 1 hour at 100,000 g, and the supernatant was mixed for 2 hours with 3 mL of anti-FLAG M2 Affinity Agarose Gel (Sigma). The resin was collected by centrifugation, washed 4 times with 10 mL Buffer B (25 mM Tris-Cl pH7.5, 10% glycerol, 0.5 mM EDTA, 75 mM KCl, 0.01% IGEPAL, 1 mM DTT), followed by protein elution with 300 mg/ml 3xFlag peptide (APExBIO) in 10 mL buffer B. The eluate was mixed with 1.5 mL of nickel-NTA resin (QIAGEN) for 2 hours in Buffer B with 15 mM imidazole. The resin was collected by centrifugation, washed 4 times each with 5 mL Buffer B with 20 mM imidazole, followed by protein elution with 200 mM imidazole in 3 mL buffer B. The eluate was concentrated to 500 μl in a 2 mL 100 kDA Centrifugal Filter (Amicon) and subjected to size exclusion chromatography on a Superdex 200 Increase GL column (GE) on an Akta FPLC system in Buffer B. Fractions containing FANCI-FANCD2 heterodimer (~300 KDa) were pooled, concentrated in a 15 mL 100 kDA Centrifugal Filter (Amicon), and stored in 3 ml aliquots at −80°C. The I(KKEE)/D2 and I(R1285X)/D2 mutant complexes were expressed and purified using the same procedure. MBP-FANCL and UBE2T were purified from E. coli Rosetta(DE3) pLysS (Novagen) as previously described (Longerich et al., 2014; Longerich et al., 2009). UBE1 and HA-ubiquitin were purchased from Boston Biochem.

The chicken FANCI-FANCD2 complex was prepared as described (Sato et al., 2012) with modifications using expression plasmids provided by the Kurumizaka laboratory. In brief, His-tagged FANCI and FANCD2 were expressed separately from Rosetta(DE3) pLysS cells grown in LB. When culture reached OD600 of 0.8 at 37°C, protein expression was induced by addition of 0.5 mM Isopropyl b-D-1-thiogalactopyranoside (IPTG), followed by overnight growth at 16°C. Cells were harvested by centrifugation and lysed in Buffer C (50 mM Tris HCl, pH 8.0, 10% Glycerol, 0.5 M NaCl, 12 mM Imidazole, 5 mM BME, 1 mM PMSF). Protein purification included Nickel affinity chromatography (QIAGEN) in Buffer C, followed by size exclusion chromatography on Superdex 200 Increase GL column on an Akta FPLC system in Buffer C plus 0.2 M NaCl without imidazole. Peak fractions with monomer size for FANCI and FANCD2 were assessed on 7.5% SDS-PAGE gel and combined to form the ID2 complex on ice for 30 minutes. The complex was then injected on Superdex 200 Increase GL column and factions with expected FANCI-FANCD2 heterodimer size were collected, concentrated in a 15 mL 100 kDA Centrifugal Filter (Amicon), aliquoted and stored at −80°C.

EMSA—The assay was conducted according to our published protocol (Longerich et al., 2009). Nuclei acid substrates used in this study are reported in Table S1. Duplex DNA, R-loop and D-loop substrates were prepared by annealing of DNA and/or RNA oligos (IDT). Following electrophoresis in a native 12% acrylamid (29:1) TBE gel at room temperature in 1X TBE buffer, substrates were eluted from gel slices by dialysis and concentrated by centrifugation using Micro Bio-Spin Chromatography Columns (Bio-Rad). All the reactions contain 10 nM ^{32}P-labeled substrates. The RNase inhibitor RNaseOUT (Thermo Fisher) was added to reactions (0.16 units/ul, 1:250) containing RNA substrates. Reactions were run on native 5% acrylamid (29:1) TBE gels at 4°C. The gels were dried onto Whatman DE81 paper and analyzed in a Personal Molecular Imager FX PhosphorImager (Bio-Rad). GelQuant.NET (http://biochemlabsolutions.com/GelQuantNET.html) software was used to quantify non-shifted substrate in each lane for calculation of the percentage of substrate bound.

ID2 *in vitro* ubiquitination assay—Reactions containing ID2 complex, HA-ubiquitin, E1, UBE2T, FANCL, and the indicated nucleic acid ligand were carried out as previously described (Longerich et al., 2014), with RNaseOUT (Thermo Fisher) being included (0.16 units/ul, 1:250) to prevent RNA degradation. Reactions were incubated overnight (~16 hours) in Figure 4C and for 7 hours in Figures 4D–4F prior to loading on 4%–15% Mini-PROTEAN TGX Precast Protein Gels (Bio-Rad). The GelQuant.NET (http://biochemlabsolutions.com/GelQuantNET.html) software was used to quantify Ub-FANCD2 and unmodified FANCD2.

QUANTIFICATION AND STATISTICAL ANALYSIS

Quantification and statistical analysis were done using Prism 7.05 (GraphPad). For DART assay, 50 cells were analyzed, and statistical significance was determined by unpaired t test. Error bars represent SEM, *p < 0.05, **p < 0.01, ***p < 0.001. For staining of RNA:DNA hybrids in FA-D2 and derivative cells, Volocity software (Perkin Elmer) was used to quantify S9.6 immunofluorescence. S9.6 signal of each time point was normalized to the

signal at 0 hour, and percentages of change were plotted. Approximately 10 cells were anaylyzed for each cell line, and statistical significance was determined by unpaired t test. Error bars represent SD. *p < 0.05, **p < 0.01, ***p < 0.001. For survival assay, crystal violet dye concentration was measured in a microplate reader (BioTek) by absorbance at 595 nm and normalized to untreated control to calculate the percentage of survival. Means were calculated from 3 replicates, error bars represent SD. For EMSA assay, signal of the non-shifted substrate in each lane was quantified using GelQuant.NET (http://biochemlabsolutions.com/GelQuantNET.html) software in order to calculate the percentage of the shifted substrates. Means were calculated from 3 replicates, error bars represent SD. For ID2 *in vitro* ubiquitination assay, signal of the ub-FANCD2 and FANCD2 bands were quantified using GelQuant.NET (http://biochemlabsolutions.com/GelQuantNET.html) software to calculate the percentage of ub-FANCD2.

Supplementary Material

Refer to Web version on PubMed Central for supplementary material.

ACKNOWLEDGMENTS

This study was supported by the NIH grants R01CA168635, RO1CA220123, P30CA054174, and U54DK106857 to G.M.K. and P.S. and GM118833 to L.L. Z.L. was supported by the Damon Runyon Cancer Research Foundation (DRG-[2253-16]), Y.T. was supported by China Scholarship Council, and T.R. was supported by the Young Investigator Award from the Alex's Lemonade Stand Foundation for Childhood Cancer.

REFERENCES

Bhatia V, Barroso SI, García-Rubio ML, Tumini E, Herrera-Moyano E, and Aguilera A (2014). BRCA2 prevents R-loop accumulation and associates with TREX-2 mRNA export factor PCID2. Nature 511, 362–365. [PubMed: 24896180]

Cantor SB, Bell DW, Ganesan S, Kass EM, Drapkin R, Grossman S, Wahrer DC, Sgroi DC, Lane WS, Haber DA, and Livingston DM (2001). BACH1, a novel helicase-like protein, interacts directly with BRCA1 and contributes to its DNA repair function. Cell 105, 149–160. [PubMed: 11301010]

Chen X, Wilson JB, McChesney P, Williams SA, Kwon Y, Longerich S, Marriott AS, Sung P, Jones NJ, and Kupfer GM (2014). The Fanconi anemia proteins FANCD2 and FANCJ interact and regulate each other's chromatin localization. J. Biol. Chem. 289, 25774–25782. [PubMed: 25070891]

Dokal I, and Vulliamy T (2010). Inherited bone marrow failure syndromes. Haematologica 95, 1236–1240. [PubMed: 20675743]

Garcia-Higuera I, Taniguchi T, Ganesan S, Meyn MS, Timmers C, Hejna J, Grompe M, and D'Andrea AD (2001). Interaction of the Fanconi anemia proteins and BRCA1 in a common pathway. Mol. Cell 7, 249–262. [PubMed: 11239454]

García-Rubio ML, Pérez-Calero C, Barroso SI, Tumini E, Herrera-Moyano E, Rosado IV, and Aguilera A (2015). The Fanconi anemia pathway protects genome integrity from R-loops. PLoS Genet. 11, e1005674. [PubMed: 26584049]

Godthelp BC, Wiegant WW, Waisfisz Q, Medhurst AL, Arwert F, Joenje H, and Zdzienicka MZ (2006). Inducibility of nuclear Rad51 foci after DNA damage distinguishes all Fanconi anemia complementation groups from D1/BRCA2. Mutat. Res. 594, 39–8. [PubMed: 16154163]

Hatchi E, Skourti-Stathaki K, Ventz S, Pinello L, Yen A, Kamieniarz-Gdula K, Dimitrov S, Pathania S, McKinney KM, Eaton ML, et al. (2015). BRCA1 recruitment to transcriptional pause sites is required for R-loop-driven DNA damage repair. Mol. Cell 57, 636–647. [PubMed: 25699710]

Hodson C, Rourke JJ, van Twest S, Murphy VJ, Dunn E, and Deans AJ (2018). FANCM-family branchpoint translocases remove co-transcriptional R-loops. bioRxiv, arXiv:248161 10.1101/248161.

Huang Y, Leung JW, Lowery M, Matsushita N, Wang Y, Shen X, Huong D, Takata M, Chen J, and Li L (2014). Modularized functions of the Fanconi anemia core complex. Cell Rep. 7, 1849–1857. [PubMed: 24910428]

Joo W, Xu G, Persky NS, Smogorzewska A, Rudge DG, Buzovetsky O, Elledge SJ, and Pavletich NP (2011). Structure of the FANCI-FANCD2 complex: Insights into the Fanconi anemia DNA repair pathway. Science 333, 312–316. [PubMed: 21764741]

Kim Y, Lach FP, Desetty R, Hanenberg H, Auerbach AD, and Smogorzewska A (2011). Mutations of the SLX4 gene in Fanconi anemia. Nat. Genet. 43, 142–146. [PubMed: 21240275]

Lan L, Nakajima S, Wei L, Sun L, Hsieh CL, Sobol RW, Bruchez M, Van Houten B, Yasui A, and Levine AS (2014). Novel method for site-specific induction of oxidative DNA damage reveals differences in recruitment of repair proteins to heterochromatin and euchromatin. Nucleic Acids Res. 42, 2330–2345. [PubMed: 24293652]

Liang CC, Li Z, Lopez-Martinez D, Nicholson WV, Vénien-Bryan C, and Cohn MA (2016). The FANCD2-FANCI complex is recruited to DNA interstrand crosslinks before monoubiquitination of FANCD2. Nat. Commun. 7, 12124.

Longerich S, San Filippo J, Liu D, and Sung P (2009). FANCI binds branched DNA and is monoubiquitinated by UBE2T-FANCL. J. Biol. Chem. 284, 23182–23186. [PubMed: 19589784]

Longerich S, Kwon Y, Tsai MS, Hlaing AS, Kupfer GM, and Sung P (2014). Regulation of FANCD2 and FANCI monoubiquitination by their interaction and by DNA. Nucleic Acids Res. 42, 5657–5670. [PubMed: 24623813]

Madireddy A, Kosiyatrakul ST, Boisvert RA, Herrera-Moyano E, Garcia-Rubio ML, Gerhardt J, Vuono EA, Owen N, Yan Z, Olson S, et al. (2016). FANCD2 Facilitates Replication through Common Fragile Sites. Mol. Cell 64, 388–04. [PubMed: 27768874]

Nalepa G, and Clapp DW (2018). Fanconi anaemia and cancer: An intricate relationship. Nat. Rev. Cancer 18, 168–185. [PubMed: 29376519]

Nguyen HD, Yadav T, Giri S, Saez B, Graubert TA, and Zou L (2017). Functions of replication protein A as a sensor of R loops and a regulator of RNaseH1. Mol. Cell 65, 832–847. [PubMed: 28257700]

Okamoto Y, Iwasaki WM, Kugou K, Takahashi KK, Oda A, Sato K, Kobayashi W, Kawai H, Sakasai R, Takaori-Kondo A, et al. (2018). Replication stress induces accumulation of FANCD2 at central region of large fragile genes. Nucleic Acids Res. 46, 2932–2944. [PubMed: 29394375]

Rajendra E, Oestergaard VH, Langevin F, Wang M, Dornan GL, Patel KJ, and Passmore LA (2014). The genetic and biochemical basis of FANCD2 monoubiquitination. Mol. Cell 54, 858–869. [PubMed: 24905007]

Santos-Pereira JM, and Aguilera A (2015). R loops: New modulators of genome dynamics and function. Nat. Rev. Genet. 16, 583–597. [PubMed: 26370899]

Sato K, Toda K, Ishiai M, Takata M, and Kurumizaka H (2012). DNA robustly stimulates FANCD2 monoubiquitylation in the complex with FANCI. Nucleic Acids Res. 40, 4553–4561. [PubMed: 22287633]

Schwab RA, Nieminuszczy J, Shah F, Langton J, Lopez Martinez D, Liang CC, Cohn MA, Gibbons RJ, Deans AJ, and Niedzwiedz W (2015). The Fanconi anemia pathway maintains genome stability by coordinating replication and transcription. Mol. Cell 60, 351–361. [PubMed: 26593718]

Skourti-Stathaki K, and Proudfoot NJ (2014). A double-edged sword: R loops as threats to genome integrity and powerful regulators of gene expression. Genes Dev. 28, 1384–1396. [PubMed: 24990962]

Sollier J, Stork CT, García-Rubio ML, Paulsen RD, Aguilera A, and Cimprich KA (2014). Transcription-coupled nucleotide excision repair factors promote R-loop-induced genome instability. Mol. Cell 56, 777–785. [PubMed: 25435140]

Taniguchi T, Garcia-Higuera I, Andreassen PR, Gregory RC, Grompe M, and D'Andrea AD (2002). S-phase-specific interaction of the Fanconi anemia protein, FANCD2, with BRCA1 and RAD51. Blood 100, 2414–2420. [PubMed: 12239151]

Teng Y, Yadav T, Duan M, Tan J, Xiang Y, Gao B, Xu J, Liang Z, Liu Y, Nakajima S, et al. (2018). ROS-induced R loops trigger a transcription-coupled but BRCA1/2-independent homologous recombination pathway through CSB. Nat. Commun. 9, 4115. [PubMed: 30297739]

Tripathi K, Mani C, Clark DW, and Palle K (2016). Rad18 is required for functional interactions between FANCD2, BRCA2, and Rad51 to repair DNA topoisomerase 1-poisons induced lesions and promote fork recovery. Oncotarget 7, 12537–12553. [PubMed: 26871286]

van Twest S, Murphy VJ, Hodson C, Tan W, Swuec P, O'Rourke JJ, Heierhorst J, Crismani W, and Deans AJ (2017). Mechanism of ubiquitination and deubiquitination in the Fanconi anemia pathway. Mol. Cell 65, 247–259. [PubMed: 27986371]

Wang X, Andreassen PR, and D'Andrea AD (2004). Functional interaction of monoubiquitinated FANCD2 and BRCA2/FANCD1 in chromatin. Mol. Cell. Biol. 24, 5850–5862. [PubMed: 15199141]

Wei L, Nakajima S, Böhm S, Bernstein KA, Shen Z, Tsang M, Levine AS, and Lan L (2015). DNA damage during the G0/G1 phase triggers RNA-templated, Cockayne syndrome B-dependent homologous recombination. Proc. Natl. Acad. Sci. USA 112, E3495–E3504. [PubMed: 26100862]

Wilson TE, Arlt MF, Park SH, Rajendran S, Paulsen M, Ljungman M, and Glover TW (2015). Large transcription units unify copy number variants and common fragile sites arising under replication stress. Genome Res. 25, 189–200. [PubMed: 25373142]

Xia B, Dorsman JC, Ameziane N, de Vries Y, Rooimans MA, Sheng Q, Pals G, Errami A, Gluckman E, Llera J, et al. (2007). Fanconi anemia is associated with a defect in the BRCA2 partner PALB2. Nat. Genet. 39, 159–161. [PubMed: 17200672]

Yamamoto KN, Kobayashi S, Tsuda M, Kurumizaka H, Takata M, Kono K, Jiricny J, Takeda S, and Hirota K (2011). Involvement of SLX4 in interstrand cross-link repair is regulated by the Fanconi anemia pathway. Proc. Natl. Acad. Sci. USA 108, 6492–6496. [PubMed: 21464321]

Yu K, Chedin F, Hsieh CL, Wilson TE, and Lieber MR (2003). R-loops at immunoglobulin class switch regions in the chromosomes of stimulated B cells. Nat. Immunol. 4, 442–451. [PubMed: 12679812]

Highlights

- FANCD2 colocalizes with co-transcriptional R-loops in human cells
- Human FANCI-FANCD2 robustly binds ssRNA, but not RNA:DNA hybrids
- Human FANCI-FANCD2 binds R-loops via the displaced ssDNA strand and ssRNA tail
- ssRNA and R-loop can stimulate robust FANCI-FANCD2 monoubiquitination

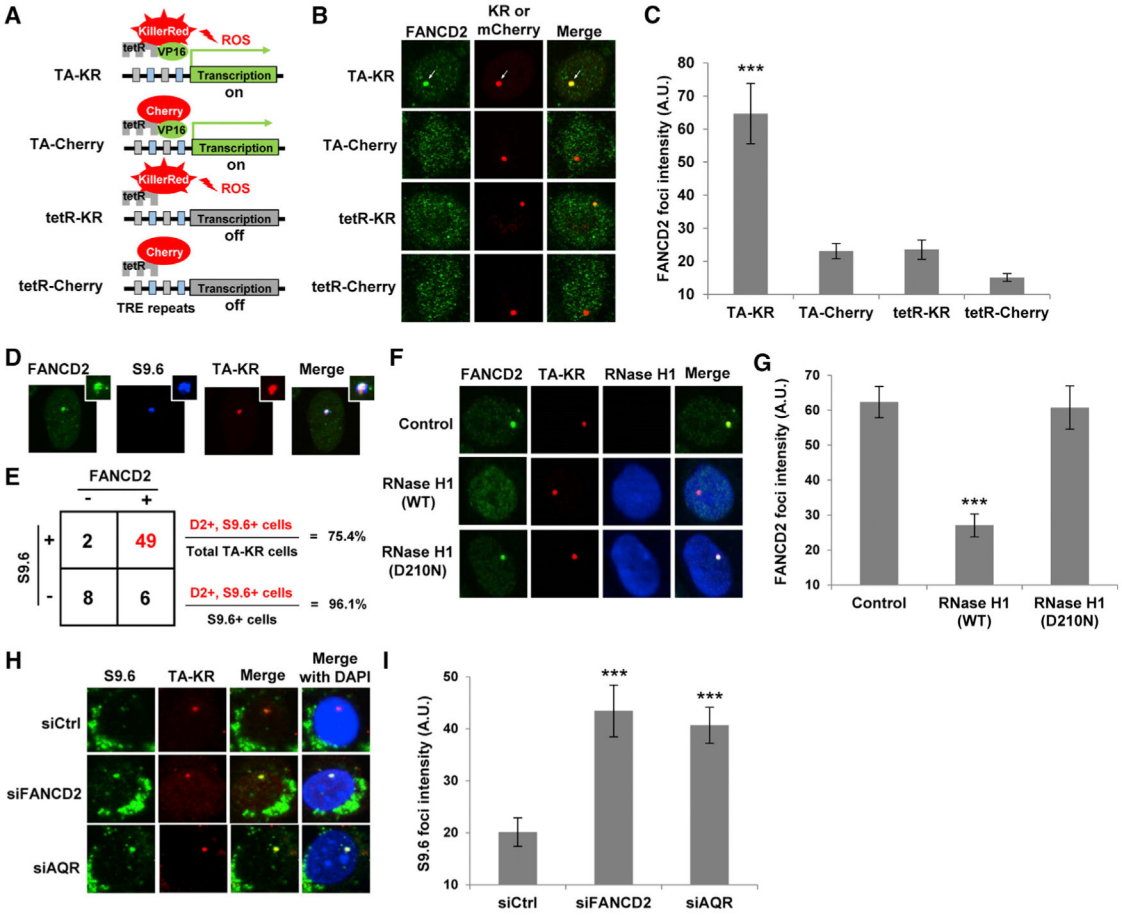

Figure 1. FANCD2 Co-localizes with R-Loop-Enriched Foci at an Actively Transcribed Genomic Site

(A) Schematic diagram of the DART system.

(B) Immunostaining of FANCD2 in four cell lines expressing different fusion effector proteins in a DART assay. FANCD2 localizes to the KR foci in presence of ROS-induced DNA damage and active transcription.

(C) Quantification of FANCD2 foci intensity at the TRE locus in (B).

(D) Colocalization of FANCD2 and S9.6 foci at the TRE locus in TA-KR positive cells.

(E) Numbers of TA-KR positive cells with or without S9.6 and FANCD2 foci at the TRE locus. Percentages of S9.6, FANCD2 foci double-positive cells over total examined cells and over S9.6 positive cells are shown.

(F) Overexpression of wild-type or nuclease-dead D210N mutant of RNase H1 in TA-KR positive cells. Wild-type RNase H1 expression diminished FANCD2 signal.

(G) Quantification of FANCD2 foci intensity at the TRE locus in (F).

(H) siRNA depletion of FANCD2 or AQR increased S9.6 foci intensity in a DART assay.

(I) Quantification of S9.6 foci intensity at the TRE locus in (H).

For (C), (G), and (I), n = 50 cells, unpaired t test; error bars represent SEM. *p < 0.05, **p < 0.01, ***p < 0.001.

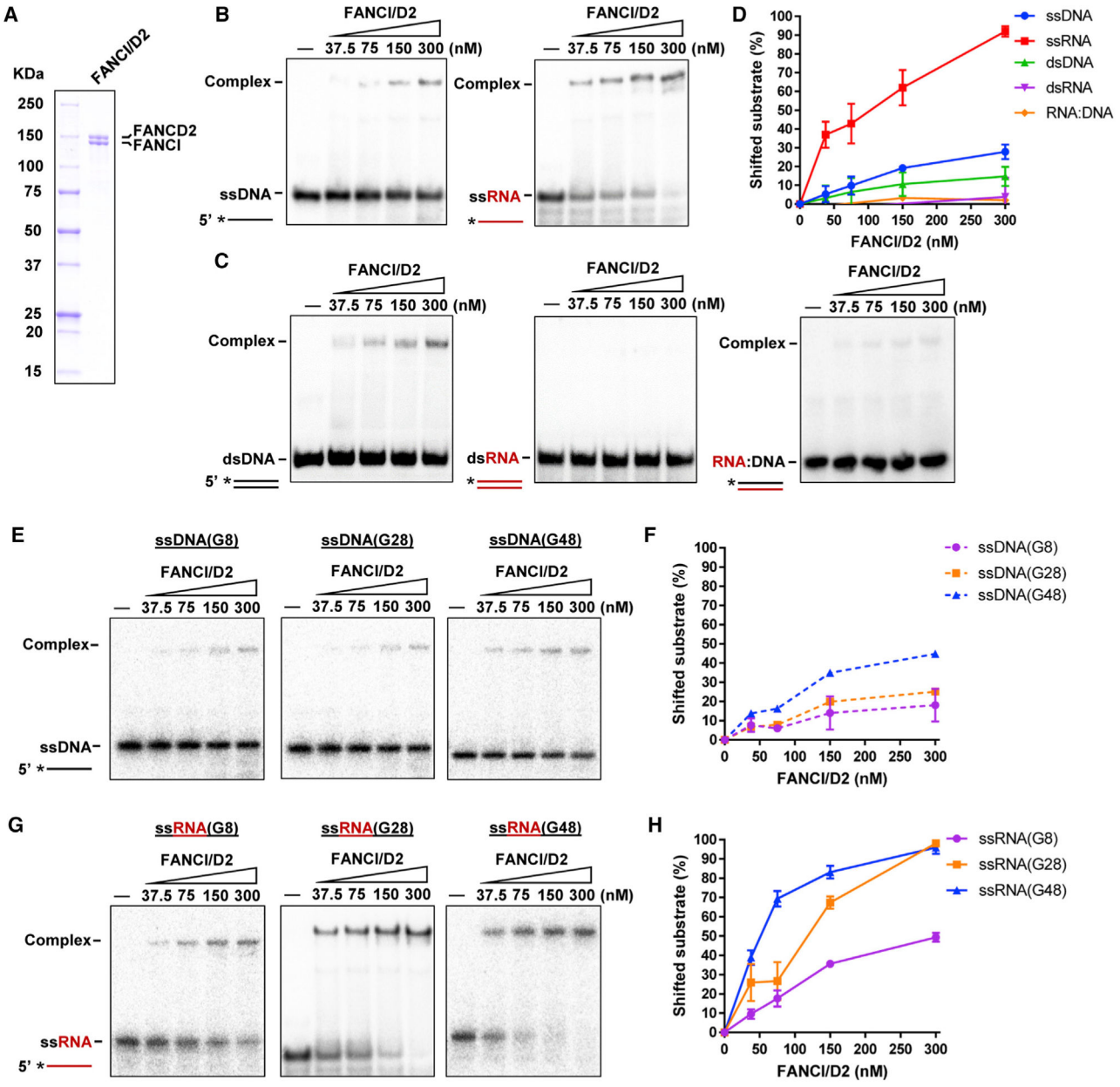

Figure 2. Recombinant ID2 Complex Preferentially Binds Single-Stranded and Guanine-Rich RNA

(A) Purified ID2 heterodimer proteins run on SDS-PAGE and stained with Coomassie Blue.

(B) EMSA showing binding of ssDNA and ssRNA by recombinant ID2.

(C) EMSA showing binding of dsDNA, dsRNA, and RNA:DNA hybrids by recombinant ID2.

(D) Quantification of shifted nucleic acid substrates in (B) and (C).

(E) EMSA showing binding of ssDNA substrates with different guanine content (8%, 28%, or 48%) by recombinant ID2.

(F) Quantification of shifted substrates in (E).

(G) EMSA showing binding of ssRNA substrates with different guanine content (8%, 28%, or 48%) by recombinant ID2.

(H) Quantification of shifted substrates in (G).

For (D), (F), and (H), means were calculated from 3 replicates; error bars represent SD.

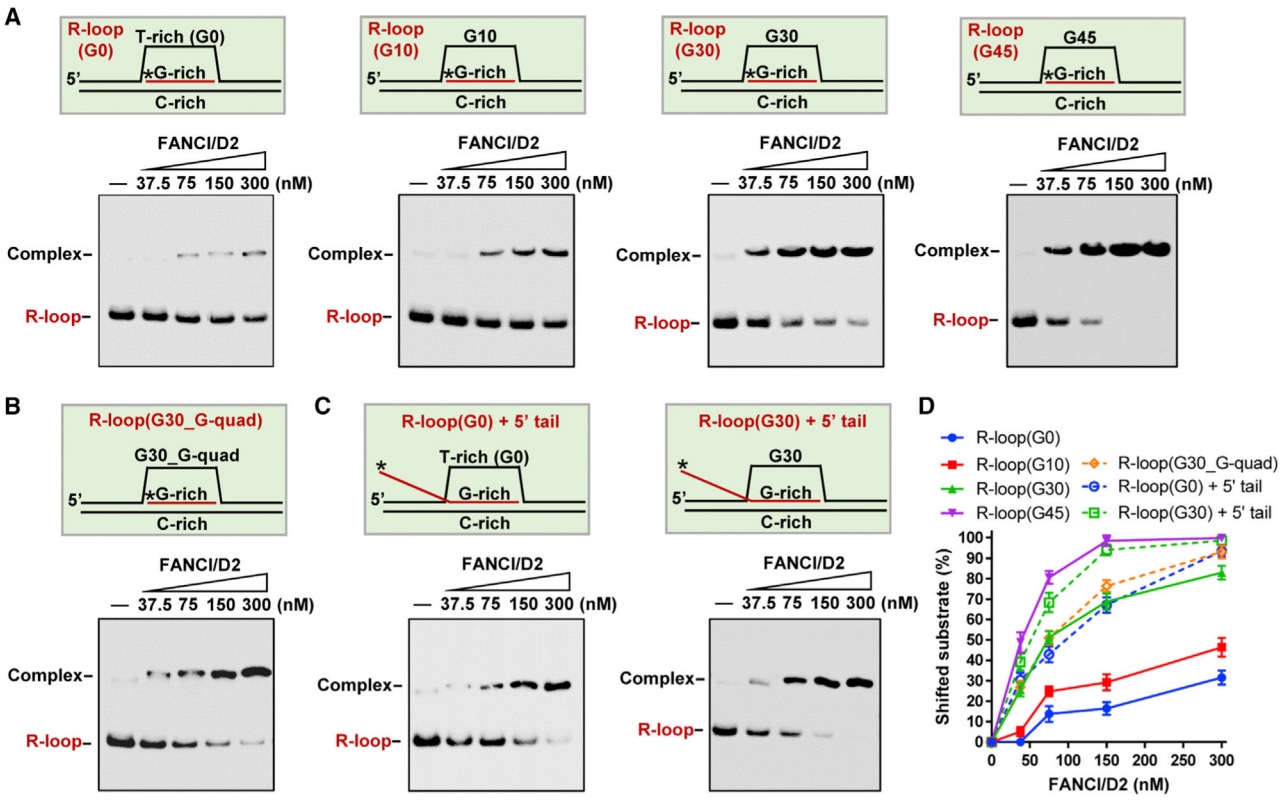

Figure 3. Human ID2 Binds the Displaced ssDNA Strand and ssRNA Tail in R-Loops

(A) EMSA showing ID2 binding of R-loop substrates carrying displaced strands with variable guanine content.

(B) EMSA showing ID2 binding of an R-loop substrate with G-quadruplex forming sequence in the displaced ssDNA strand.

(C) EMSA showing ID2 binding of R-loop substrates with a 40-nt 5′ ssRNA tail.

(D) Quantification of shifted substrates in (A)–(C); means were calculated from 3 replicates; error bars represent SD.

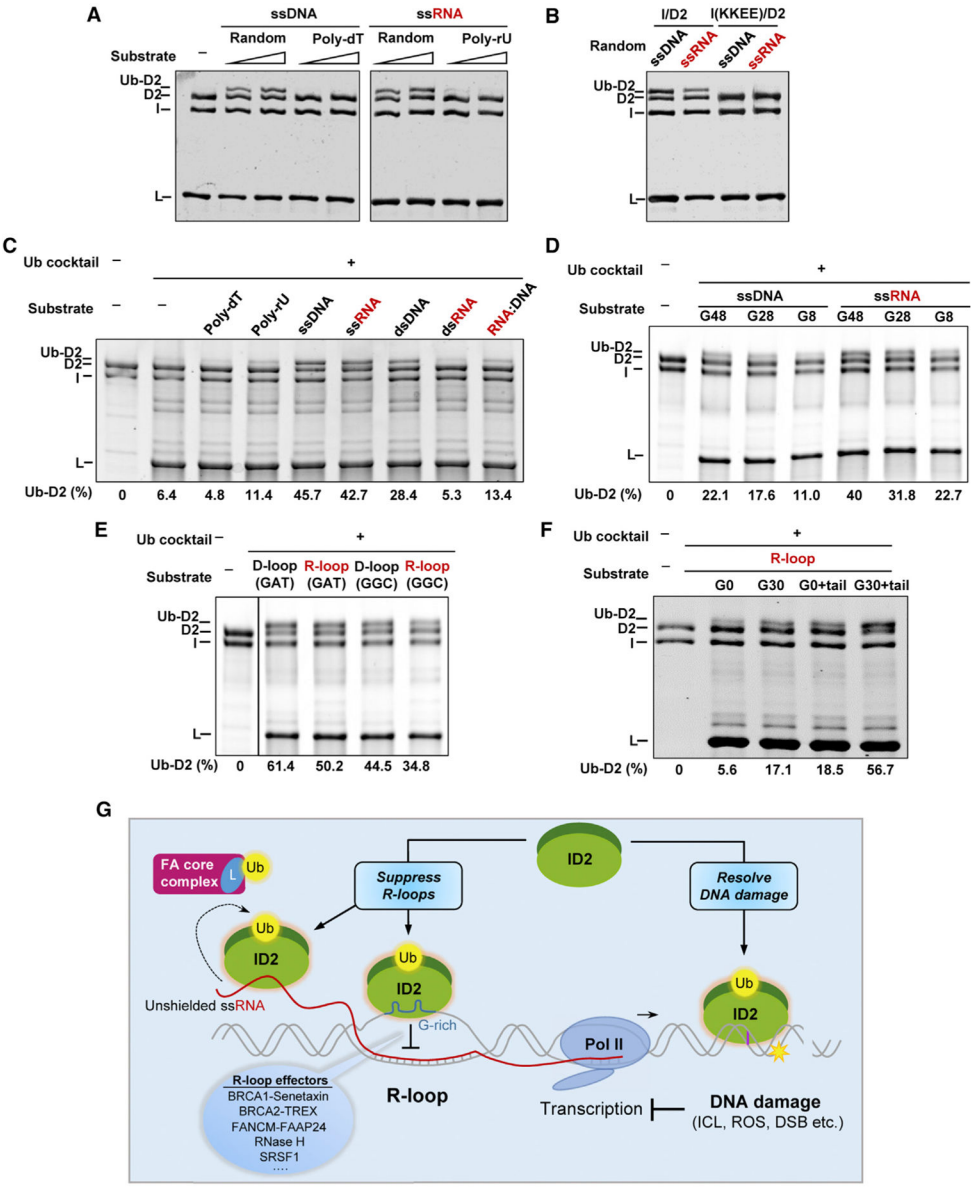

Figure 4. RNA and R-Loop Stimulate FANCD2 Monoubiquitination

(A) *In vitro* ubiquitination reaction of recombinant ID2 with either ssDNA or ssRNA substrates. FANCD2 was ubiquitinated maximally in presence of random sequence of ssRNA or ssDNA and ubiquitination was abrogated by T or U-rich nucleic acids.

(B) DNA and RNA binding mutant FANCI(KKEE)/D2 complex failed to be ubiquitinated.

(C) Comparison of ID2 ubiquitination efficiency using various nucleic acids substrates with different binding affinity. ssRNA conferred the most ubiquitination.

(D) Comparison of ID2 ubiquitination efficiency using nucleic acids substrates with different guanine content. Nucleic acid with the highest guanine content conferred the most ubiquitination.

(E) Comparison of ID2 ubiquitination efficiency using two configurations of D-loops and R-loops. D- and R-loops with guanine-containing single-strand DNA (ssDNA) supported ID2 ubiquitination similarly.
(F) Comparison of ID2 ubiquitination efficiency using different R-loop substrates. R-loops with guanine-containing ssDNA and ssRNA tail supported ID2 ubiquitination with the highest efficiency. For (C)–(F), percentage of ubiquitinated FANCD2 is calculated by the intensity of the Ub-D2 band over total intensity of the Ub-D2 and D2 bands.
(G) Model of R-loop binding and its stimulated monoubiquitination of FANCI-FANCD2 in response to DNA damage-induced transcriptional perturbation.

KEY RESOURCES TABLE

REAGENT or RESOURCE	SOURCE	IDENTIFIER
Antibodies		
Rabbit polyclonal anti-FANCD2	Abcam	Cat# ab2187; RRID:AB_302885
Rabbit polyclonal anti-FANCD2	Bethyl Laboratories	Cat# A302-174A; RRID:AB_1659803
Mouse monoclonal anti-FANCD2	Santa Cruz Biotechnology	Cat# sc-20022; RRID:AB_2278211
Rabbit polyclonal anti-FANCI	Bethyl Laboratories	Cat# A301-254A; RRID:AB_890616
Rabbit polyclonal anti-RNase H1	Abcam	Cat# ab229078
Mouse monoclonal anti-Ku86	Santa Cruz Biotechnology	Cat# sc-5280; RRID:AB_672929
Mouse monoclonal S9.6	Kerafast or purify from mouse BALB/c cells	Cat# ENH001; RRID:AB_2687463
mouse monoclonal anti-HA	Roche	Cat# 11583816001; RRID:AB_514505
Goat anti-Mouse IgG (H+L) Cross-Adsorbed Secondary Antibody, Alexa Fluor 488	Thermo Fisher	Cat# A-11001; RRID:AB_2534069
Goat anti-Mouse IgG (H+L) Cross-Adsorbed Secondary Antibody, Alexa Fluor 405	Thermo Fisher	Cat# A-31553; RRID:AB_221604
Goat anti-Rabbit IgG (H+L) Cross-Adsorbed Secondary Antibody, Alexa Fluor 488	Thermo Fisher	Cat# A-11008; RRID:AB_143165
Goat anti-Mouse IgG (H+L) Cross-Adsorbed Secondary Antibody, Alexa Fluor 555	Thermo Fisher	Cat# A-21422; RRID:AB_141822
ECL Rabbit IgG, HRP-linked whole Ab (from donkey)	Amersham Health	Cat# NA934; RRID:AB_772206
ECL Mouse IgG, HRP-linked whole Ab (from sheep)	Amersham Health	Cat# NA931; RRID:AB_772210
Bacterial and Virus Strains		
Rosetta(DE3) pLysS	Novagen	Cat# 70956
NEB 5-alpha Competent *E. coli* (High Efficiency)	NEB	Cat# C2987I
Chemicals, Peptides, and Recombinant Proteins		
Mitomycin C (MMC)	Sigma	Cat# M4287
Crystal Violet	Sigma	Cat# C0775
Sodium bisulfite	Sigma	Cat# 243973
High Capacity Streptavidin Agarose	Pierce	Cat# 20357
3x Flag peptide	APExBIO	Cat# A6001
anti-FLAG M2 Affinity Agarose Gel	Sigma	Cat# A2220
Ni-NTA Agarose	QIAGEN	Cat# 30250
Imidazole	Sigma	Cat# I5513
Recombinant human FANCI	This paper	N/A
Recombinant human FANCI-FANCD2	This paper	N/A
Recombinant chicken FANCI	This paper	N/A
Recombinant chicken FANCD2	This paper	N/A
Recombinant chicken FANCI-FANCD2	This paper	N/A
Recombinant human FANCL	Longerich et al., 2014	N/A
Recombinant human UBE2T	Longerich et al., 2014	N/A
UBE1	Boston Biochem	Cat# E-305

REAGENT or RESOURCE	SOURCE	IDENTIFIER
HA-ubiquitin	Boston Biochem	Cat# U-110
RNaseOUT Recombinant Ribonuclease Inhibitor	Thermo Fisher	Cat# 10777019
Critical Commercial Assays		
Bradford Protein Assay Kit	Pierce	Cat# 23200
Supersignal West Pico Kit	Pierce	Cat# 34078
NAb Protein A/G Spin Kit	Thermo Fisher	Cat# 89980
Bac-to-Bac Baculovirus Expression System	Thermo Fisher	Cat# 10359016
Experimental Models: Cell Lines		
Human: PD20 (FA-D2) cells	Coriell Institute	GM16756
Human: PD20 FANCD2 complemented cell lines	This paper	N/A
Human: U2OS TRE cells	Lan et al., 2014	N/A
Mouse: S9.6 hybridoma cell line	ATCC	HB-8730
Insect: Sf9 cells	Thermo Fisher	Cat# 11496015
Insect: High Five cells	Thermo Fisher	Cat# B85502
Oligonucleotides		
Refer to Table S1	This paper	N/A
Recombinant DNA		
pMMP-Flag-FANCD2 and pMMP-Flag-K561R	This paper	N/A
pEGFP-N1-RNASEH1	Gift of James Manley, Columbia University	N/A
TA-KR, tetR-KR, TA-Cherry and tetR-Cherry plasmids	Lan et al., 2014	N/A
HA-RNase H1 expressing plasmids	Nguyen et al., 2017	N/A
pFastBac[6xHis-TEV-FANCI]	Longerich et al., 2014	N/A
pFastBac[3xFlag-FANCD2]	Longerich et al., 2014	N/A
pET-15 b[6xHis-chicken.FANCI]	Sato et al., 2012	N/A
pET-15 b[6xHis-chicken.FANCD2]	Sato et al., 2012	N/A
Software and Algorithms		
Volocity	Perkin Elmer	N/A
ImageJ 1.50i	NIH	N/A
GelQuant.NET 1.8.2	biochemlabsolutions.com	http://biochemlabsolutions.com/GelQuantNET.html
Prism 7.0.5	GraphPad	N/A